DINAME 2023 - Proceedings of the XIX International Symposium on Dynamic Problems of Mechanics,
A.S. De Paula, A.T. Fabro and M.R. Machado (Editors), ABCM.
Pirenópolis, Go, Brazil, February 26th to March 3rd, 2023

Time domain aeroelastic analysis of the Pre-Pazy and Pazy Wings

João Pedro Tavares Pereira dos Santos[1], Guilherme Ribeiro Begnini[2] and Flávio Donizeti Marques[1]

[1] Mechanical Engineering Department, São Carlos Engineering School of University of São Paulo, Avenida Trabalhador são-carlense, 400 - Parque Arnold Schimidt, 13566-590, São Carlos/SP, Brazil

[2] Mechanical Engineering Department, Polytechnic School of Federal University of Bahia, R. Prof. Aristídes Novis, 2 - Federação, 40210-630, Salvador/BA, Brazil

Abstract: Aeroelastic analyses are performed either in time or frequency domains. Frequency domain analyses have the advantage of providing a fast computation of the flutter speed and are more widespread. Their results are presented in the so-called velocity-damping-frequency (V-g-f) plots, which shows the evolution of the natural frequency and damping ratio of each vibration mode as a function of airspeed. This way, the flutter speed (where zero damping occurs) can be determined with precision. On the other hand, time domain analyses allow the inclusion of different types of nonlinearities in the simulations, with the price of being more time consuming. Their results consist of time histories whose vibration amplitudes should be visually inspected to find a constant amplitude situation (zero damping condition). This paper presents a time domain aeroelastic analysis of the Pre-Pazy and Pazy wings, which are being investigated by the Large Deflection Working Group of the Third Aeroelastic Prediction Workshop. Time domain results are then used to generate V-g-f plots through modal parameter identification. For the structural dynamics modeling the classical beam theory (Euler-Bernoulli) has been applied, and the natural frequencies and mode shapes were obtained via the Finite Element Method (FEM). For the aerodynamic modeling, the Unsteady Vortex Lattice Method (UVLM) was used, which is a three-dimensional aerodynamic model based on a potential flow formulation. The structural and aerodynamic models are coupled using a surface splines interpolation method, and the equation of motion is solved iteratively on a time-domain basis, applying a predictor-corrector method. The frequency spectrum of each time response serves as input to the modal parameter identification method, which uses the Least Squares Complex Frequency estimator (LSCF). The structural and aeroelastic results of those wings are evaluated. It was possible to obtain very clear V-g-f plots, with a precise identification of flutter speeds, for all tested cases. The influence of the wing skin on the flutter speed results was assessed.

Keywords: Aeroelasticity, Unsteady Vortex Lattice Method, Finite Element Method, System Identification, Flutter

INTRODUCTION

On the latest years, in searching for more efficiency and less fuel consumption, longer and more flexible wings have been developed, which reduces the induced drag. These characteristics increase the importance of aeroelastic analysis of these structures, which allows to determine how the oscillatory behavior will be in the presence of air flow. For aeroelastic analysis, two distinct mathematical models must be coupled: one to represent the structural dynamics and other to represent the aerodynamics of the wing. The structural dynamics model aims to determine the natural frequencies and vibrational mode shapes, and the aerodynamic model aims to determine the loads acting on the structure. Coupling those two models, it's possible to solve the dynamic equations of motion and predict the oscillatory behaviour of the wing.

The Large Deflection Working Group of the Third Aeroelastic Prediction Workshop (AePW-3) focuses on the analysis of those highly flexible wings. Aiming to supply the necessity of experimental data related to the modeling of those wings, two wings were proposed, the Pre-Pazy wing and the Pazy wing (Avin et al., 2021), both tested on a wing tunnel. They have been used as a benchmark case to facilitate the comparison and validation of different aeroelastic models. Related to those wings, Ritter, Hilger and Zimmer (2021) studied the static response and the flutter mechanisms coupling a nonlinear FEM model on the MSC Nastran with the Unsteady Vortex Lattice Method. Drachinsky and Raveh (2021) proposed for the static and flutter analysis a structural model based on the Modal Rotation Method (MRM). Goizueta et al. (2021) compared Drachinsky and Raveh (2021) results, with the ones obtained by applying the SHARPy code (del Carre et al., 2019). Riso and Cesnik (2021) developed a reduced-order model, coupling a beam model based on the deformations with a strip aerodynamic model.

The aeroelastic model proposed here to analyze the Pre-Pazy and Pazy wings is the time domain model developed by Benini et al. (2004), and the time histories are used to generate the velocity-damping-frequency (V-g-f) plots, which allows the visualization of the evolution of the natural frequency and damping ratio of each vibration mode as a function of the airspeed, through modal parameter identification. For the structural dynamics modeling, the Euler-Bernoulli beam mode has been applied. The Unsteady Vortex Lattice Method

(UVLM) (Katz and Plotkin, 1991) was applied for the aerodynamic modeling. Both models are coupled together using a surface splines interpolation method, and the equation of motion is solved iteratively on a time-domain basis, applying a predictor-corrector method. The frequency spectrum of each time response serves as input to the model parameter identification method, which uses the Least Squares Complex Frequency estimator (LSCF) (Guillaume et al., 2003).

AEROELASTIC MODEL

For the structural part of the aeroelastic analysis, the Finite Element Method was applied considering Euler-Bernoulli beam elements on the discretization. The beam element has 12 DOF and the theory regarding this beam formulation is presented by Cook and Saunders (1984), Craig and Kurdila (2006), Reddy (2019) and Katsikadelis (2020).

The wing structural response is assumed to be linear and without internal damping. The equation of motion for the structure is discretized in N degrees of freedom (DOF) and shown in Eq. (1), where $\boldsymbol{M}$ and $\boldsymbol{K}$ are $N \times N$ matrices, representing the mass and stiffness properties, and $\boldsymbol{x}(t)$, $\ddot{\boldsymbol{x}}(t)$ and $\boldsymbol{L}(\boldsymbol{x}, \dot{\boldsymbol{x}}, \boldsymbol{t})$ are $N \times 1$ vectors, representing the displacements, accelerations and external (aerodynamic) forces.

$$\boldsymbol{M}\ddot{\boldsymbol{x}}(t) + \boldsymbol{K}\boldsymbol{x}(t) = \boldsymbol{L}(\boldsymbol{x}, \dot{\boldsymbol{x}}, \boldsymbol{t}) \tag{1}$$

The natural frequencies (ω_r) and mode shapes ($\boldsymbol{\phi}_r$) of the undamped multiple degree of freedom system are obtained by solving the following eigenvalue problem

$$\left(\boldsymbol{K} - \omega_r^2 \boldsymbol{M}\right) \boldsymbol{\phi}_r = \boldsymbol{0} \tag{2}$$

The mode shapes can be arranged in a matrix, as seen in Eq. (3). This matrix is called modal matrix and is used as a coordinate transformation matrix, according to Eq. (4), where $\boldsymbol{\eta}(t)$ represents the structural displacements in a modal domain and can be interpreted as a vector of coefficients which determines the influence of each mode shape in the physical structural response.

$$\boldsymbol{\Phi} = [\boldsymbol{\phi}_1\, \boldsymbol{\phi}_2\, \boldsymbol{\phi}_3 \cdots \boldsymbol{\phi}_N] \tag{3}$$

$$\boldsymbol{x}(t) = \boldsymbol{\Phi}\boldsymbol{\eta}(t) = \sum_{r=1}^{N} \boldsymbol{\phi}_r \boldsymbol{\eta}_r(t) \tag{4}$$

As $\boldsymbol{\Phi}$ is constant in time, it's possible to write

$$\ddot{\boldsymbol{x}}(t) = \boldsymbol{\Phi}\ddot{\boldsymbol{\eta}}(t) \tag{5}$$

Substituting Eq. (4) and Eq. (5) in Eq. (1) and pre-multiplying both sides by $\boldsymbol{\Phi}^T$, yields Eq. (6), where $\boldsymbol{M}_m = \boldsymbol{\Phi}^T \boldsymbol{M} \boldsymbol{\Phi}$ and $\boldsymbol{K}_m = \boldsymbol{\Phi}^T \boldsymbol{K} \boldsymbol{\Phi}$ are named modal mass and modal stiffness matrices, respectively.

$$\boldsymbol{M}_m \ddot{\boldsymbol{\eta}}(t) + \boldsymbol{K}_m \boldsymbol{\eta}(t) = \boldsymbol{\Phi}^T L(x, \dot{\boldsymbol{x}}, t) \tag{6}$$

Due to the orthogonality properties of the mode shapes, one can prove that the matrices $\boldsymbol{M}_m$ and $\boldsymbol{K}_m$ are diagonal matrices. In addition, it is possible to normalize the eigenvectors in a form that $\boldsymbol{M}_m = I$, and then the division of both sides of Eq. (6) by the matrix $\boldsymbol{M}_m$ yields Eq. (7), where ω^2 is a diagonal matrix containing the squared natural frequencies. In order to simplify the solution of Eq. (7), it is useful to consider only a few natural modes to describe the structural response.

$$\ddot{\boldsymbol{\eta}}(t) + \boldsymbol{\omega}^2 \boldsymbol{\eta}(t) = \boldsymbol{\Phi}^T \boldsymbol{L}(\boldsymbol{x}, \dot{\boldsymbol{x}}, t) \tag{7}$$

Another important step of the aeroelastic analysis is the determination of the aerodynamic loads ($\boldsymbol{L}(\boldsymbol{x},\dot{\boldsymbol{x}},t)$). The aerodynamic model used here is the Unsteady Vortex Lattice Method (UVLM), described by Katz and Plotkin (1991), which will be discussed on the next topic. Once those loads are determined, the structural and aerodynamic models must be coupled together.

The mode shapes and the aerodynamic forces are defined using different meshes, so it is necessary to convert the aerodynamic forces to the structural points and to supply the structural displacements to the aerodynamic

points. The aerodynamic and structural points are related through a coordinate transformation matrix ($\boldsymbol{G}$), and this matrix can be applied to write the mode shapes in terms of the aerodynamic points, according to Eq. (8), where the subscript a is related to the aerodynamic points and s to the structural points (Benini et al., 2004).

$$\boldsymbol{\Phi}_a = \boldsymbol{G}\boldsymbol{\Phi}_s \tag{8}$$

Also it is possible to write the aerodynamic forces in terms of the structural points using the same coordinate transformation matrix.

$$\boldsymbol{L}_s = \boldsymbol{G}^T \boldsymbol{L}_a \tag{9}$$

Substituting Eq. (9) into Eq. (7) and making use of Eq. (8) yields Eq. (10), which represents the conversion of forces between the two meshes.

$$\ddot{\boldsymbol{\eta}}_s(t) + \omega^2 \boldsymbol{\eta}_s(t) = \boldsymbol{\Phi}_a^T \boldsymbol{L}_a \tag{10}$$

This equation is solved iteratively applying a predictor-corrector method, which is described by Benini et al. (2004), and the modal displacements ($\boldsymbol{\eta}$), that represent the wing response, are found.

UNSTEADY VORTEX LATTICE METHOD

The UVLM is an aerodynamic method based on the potential theory and on the resolutions of Laplace's equations. This method is a extremely useful tool to solve three-dimensional potential flow problems and to represent lifting surfaces. This surfaces, combined with the wake, are modelled through vortex rings elements.

The lifting surface, here the wing, is discretized in rectangular panels along the curvature line of the airfoil. Each vortex ring is associated to one of those panels. The rings connected to the lifting surface are called bound vortex rings. With the movement of the wing, more vortex rings are formed and the wake arises. Besides that, a normal vector is defined in each collocation point.

The UVLM is solved through a time iterative algorithm. New wake vortex rings are generated each time step, starting from the wing trailing edge, and the correspondent circulation values (Γ) are defined. It's important to emphasize that the circulation of the wake rings are equal to the ones of the trailing edge of the wing, which is described by

$$\Gamma_W = \Gamma_{T.E.} \tag{11}$$

To calculate the aerodynamic loads acting on the wing, it's necessary to solve the flow field, finding the circulation of the vortex rings linked to the wing panels. For this to be possible, the first step is to calculate the influence that each vortex ring exerts on the flow field, and, for this, the so-called Aerodynamic Influence Coefficients (AIC) are used. This coefficients are defined from the calculation of the induced velocity of each vortex segment of the ring on the collocation points.

The aerodynamic influence of each ring, here called a_{kl}, is defined by

$$a_{kl} = \mathbf{q}_{kl} \cdot \mathbf{n}_k \tag{12}$$

where a_{kl} is the influence of ring l on the collocation point k, $\mathbf{q}_{kl}$ is the induced velocity, found applying the Biot-Savart law, on the collocation point k by the vortex ring l and $\mathbf{n}_k$ is the normal vector of the ring k. Combining those aerodynamic influences on a matrix, the AIC matrix is defined.

$$AIC = \begin{bmatrix} a_{11} & a_{12} & \cdots & a_{1m} \\ a_{21} & a_{22} & \cdots & a_{2m} \\ \vdots & \vdots & \ddots & \vdots \\ a_{m1} & a_{m2} & \cdots & a_{mm} \end{bmatrix} \tag{13}$$

Katz and Plotkin (1991) introduced what they called the right hand side (RHS) of the equations, which are related to the components of the velocities due to the wing movement along the collocation points ($[U(t), V(t), W(t)]_k$), and to the components of the wake induced velocities ($(u_W, v_W, w_W)_k$) on that same point. The right hand side (RHS) of the equation for a collocation point k is given by

$$RHS_k = -\left[U(t)+u_W, V(t)+v_W, W(t)+w_W\right]_k \cdot \mathbf{n}_k \tag{14}$$

Once the influence coefficients and the righ hand side vectors (**RHS**) are computed, the following system of algebraic equations arises:

$$\mathbf{\Gamma} = \mathbf{AIC}^{-1}\mathbf{RHS} \tag{15}$$

The circulation of each panel is found for each time step solving Eq. (15), and the wing panels pressure distribution is determined. The methodology applied here to find this pressure distribution is described by Katz and Plotkin (1991), and is based on the non-stationary Bernoulli equation. Once the pressure distribution for each wing panel, Δp_{ij}, is determined, it's possible to calculate the lift contribution of each wing panel (Katz and Plotkin, 1991).

$$\Delta L_{ij} = \Delta p_{ij} S_{ij} \cos\alpha_{ij} \tag{16}$$

where S_{ij} is the panel area and α_{ij} the angle of attack.

Once the structural-dynamic and the aerodynamic models are defined, it's necessary to couple them to obtain the aeroelastic response of the wing. The methodology applied for the coupling of those two models is described in details by Benini et al. (2004).

MODAL PARAMETER IDENTIFICATION

As the UVLM provides the results in a time domain basis, to obtain the velocity-damping-frequency (V-g-f) plots it's necessary to apply a system identification method. This makes possible, starting from the frequency spectrum's of the time response, to obtain the natural frequencies and the respective damping ratios for each velocity. Analyzing the point where the damping ratio is null, it's possible to determine the flutter speed and frequency.

The modal parameter identification method applied in this work is the Least-Squares Complex Frequency (LSCF), described by Guillaume et al.(2003). This method is an implementation in the frequency domain of the well known Least-Squares Complex Exponential (LSCE). The main advantage of the LSCF over the LSCE, is the fact that it provides a fast stabilization, what makes it a efficient tool to find the modal parameters. All the theory involved and the numerical implementation procedure for the modal parameter identification method applied in this work are presented by Guillaume et al.(2003).

RESULTS AND DISCUSSION

The Pre-Pazy and Pazy wings are rectangular wings with the same geometry. The differences between both wings are the structural and inertia properties, which, mainly due to manufacturing aspects, are different. The general properties of those wings are shown in Table 1

Table 1 – Wing Properties and Aeroelastic Input Parameters

Structural Properties	
Semi-Span (m)	0.55
Chord (m)	0.1
Mass (kg)	0.32
Spar Material	Aluminium 7075
Spar Length (mm)	550
Spar Width (mm)	60
Spar Thickness (mm)	2.25
Tip Rod Length (mm)	300
Tip Rod Diameter (mm)	10

Aeroelastic Input Parameters	
Velocity (m/s)	10 - 80
Air Density (kg/m^3)	1.225
Chordwise Panels	4
Spanwise Panels	13
Time Step (Seconds)	0.0001
Total Iterations	30001
Total Time (Seconds)	3
Number of Modes	4

The first step for the aeroelastic analysis, is to conduct the modal analysis. Here, a linear beam structural-dynamic FEM model, developed by the authors, was applied. Riso and Cesnik (2021) provided for the AePW-3 working group the stiffness and inertia properties of the Pre-Pazy and Pazy wings discretized in fifteen beam elements, and considering each wing with and without skin, what is shown in Fig. 1, which incur in four distinct analysis scenarios.

Figure 1 – Pazy Wing

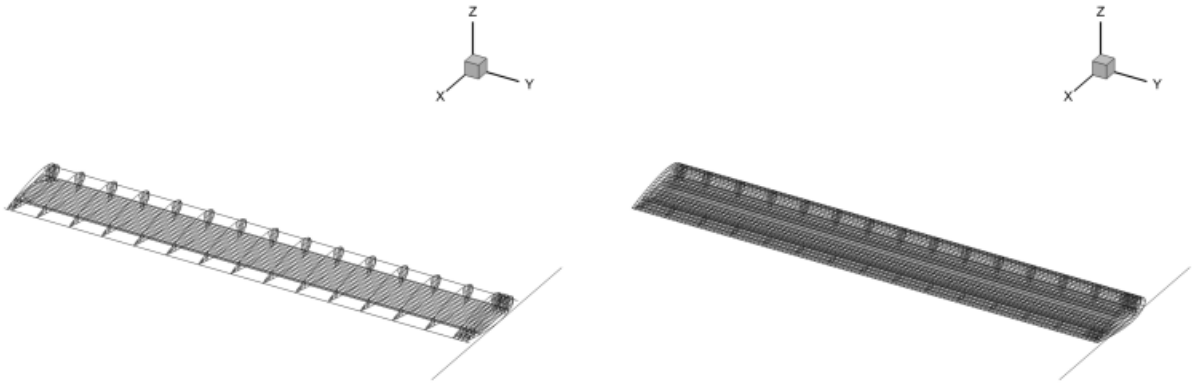

Source: Riso and Cesnik (2021)

The results obtained for the natural frequencies are compared to the ones obtained by Riso and Cesnik (2021) using the commercial software MSC Nastran. The results are presented in Table 2.

Table 2 – Modal Analysis

		Without Skin			With Skin		
		MSC Nastran (Riso and Cesnik (2021))	Present Work		MSC Nastran (Riso and Cesnik (2021))	Present Work	
	Modes	Freq. (Hz)	Freq. (Hz)	Dif. (%)	Freq. (Hz)	Freq. (Hz)	Dif. (%)
Pre-Pazy	1st Mode (OOP Bending)	4.42	4.41	-0,24%	4.67	4.66	-0.11%
	2nd Mode (OOP Bending)	29.02	29.09	0.23%	30.68	30.79	0.34%
	3rd Mode (Torsion)	41.53	41.48	-0,11%	43.57	43.55	-0.05%
	4th Mode (OOP Bending)	83.34	83.35	0.01%	87.97	88.16	0.22%
	5th Mode (IP Bending)	112.56	118.67	5.42%	112.88	119.01	5.43%
Pazy	1st Mode (OOP Bending)	4.22	4.22	0.00%	4.19	4.19	0.00%
	2nd Mode (OOP Bending)	28.28	28.42	0.50%	28.49	28.56	0.25%
	3rd Mode (Torsion)	41.55	41.52	-0.07%	41.97	41.94	-0.07%
	4th Mode (OOP Bending)	81.89	82.09	0.24%	82.92	82.71	-0.25%
	5th Mode (IP Bending)	107.74	113.72	5.55%	104.98	110.91	5.65%

The mode shapes for the Pre-Pazy and Pazy wings with skin are presented, respectively, on figures Fig. 2 and Fig. 3.

Figure 2 – Mode Shapes - Pre-Pazy Wing With Skin

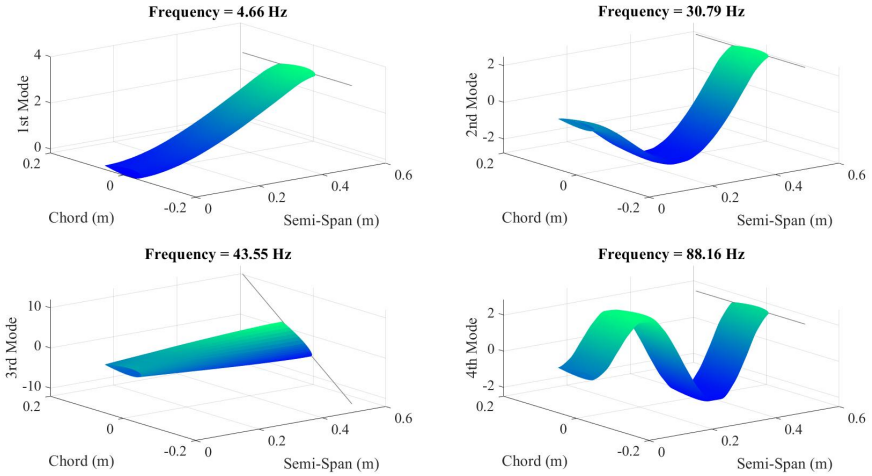

Source: Autors

Figure 3 – Mode Shapes - Pazy Wing With Skin

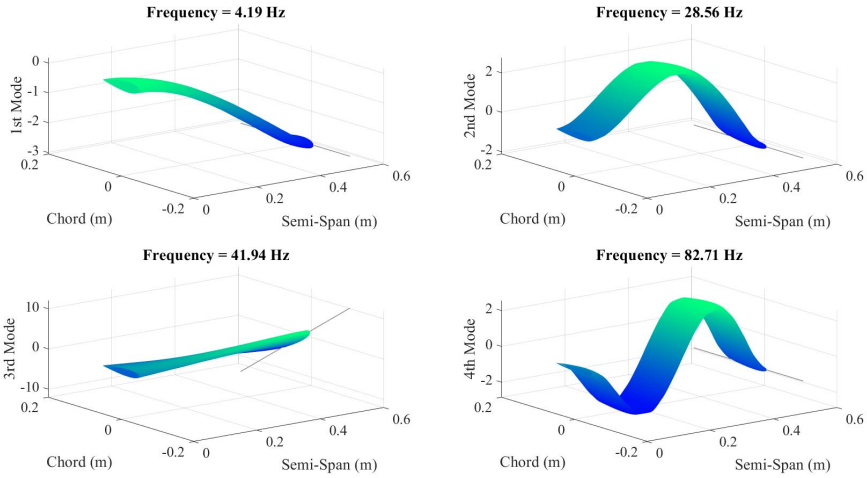

Source: Autors

Once the modal analysis was conducted, the natural frequencies and mode shapes serves as input for the aerodynamic and aeroelastic solvers. The input parameters for the aeroelastic analysis are shown in Table 1.

As the UVLM works in a time domain basis, the results obtained are the time histories of the wing modal displacements. For the Pre-Pazy and Pazy wings, each one with and without skin, the time responses and power spectrum densities (PSD) for the velocity equals to 60m/s and 70m/s are presented on Fig. 4, Fig. 5, Fig. 6 and Fig. 7.

Figure 4 – Time Response - Pre-Pazy Wing - $V = 60m/s$

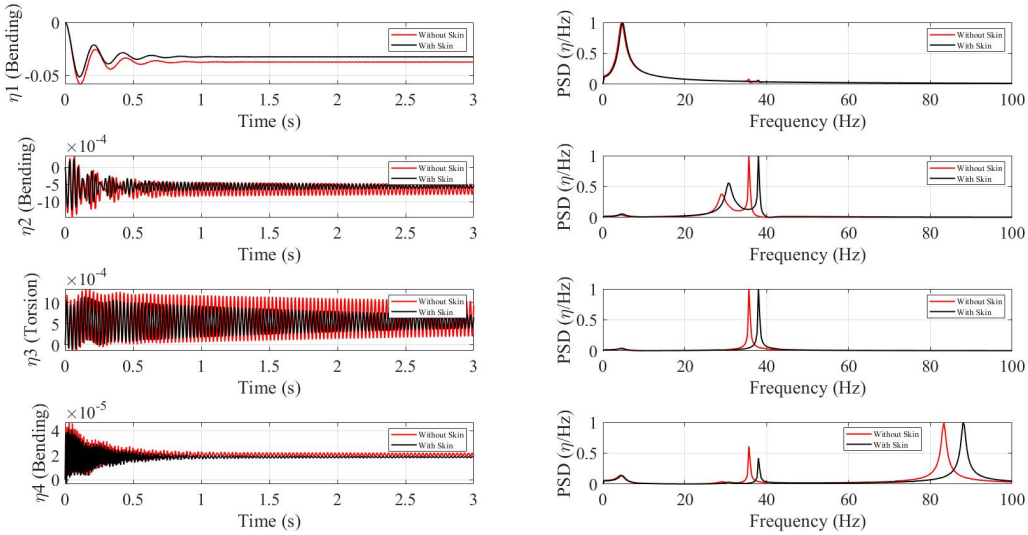

Source: Autors

From Fig. 4, Fig. 5, Fig. 6 and Fig. 7, it's possible to visualize small differences between the wings with and without skin. Also, it's possible to afirm that for both wings the flutter speed is between 60m/s and 70m/s, given that for all cases the system is unstable at 70m/s.

To assess the flutter speeds and frequencies with precision, the Least-Squares Complex Frequency (LSCF) (Guillaume et al., 2003) was applied. It provides, from the Power Spectrum Densities as inputs, the natural frequencies and damping ratios for each velocity. From this information, the velocity-damping-frequency (V-g-f) charts are obtained. Fig. 8 shows the V-g-f's for the Pre-Pazy wing and Fig. 9 for the Pazy wing.

From the V-g-f, it's possible to identify with precision the flutter speed and frequency for each wing. The results for the flutter speed are presented in Table 3, and compared with other results available in the literature.

Figure 5 – Time Response - Pre-Pazy Wing - $V = 70m/s$

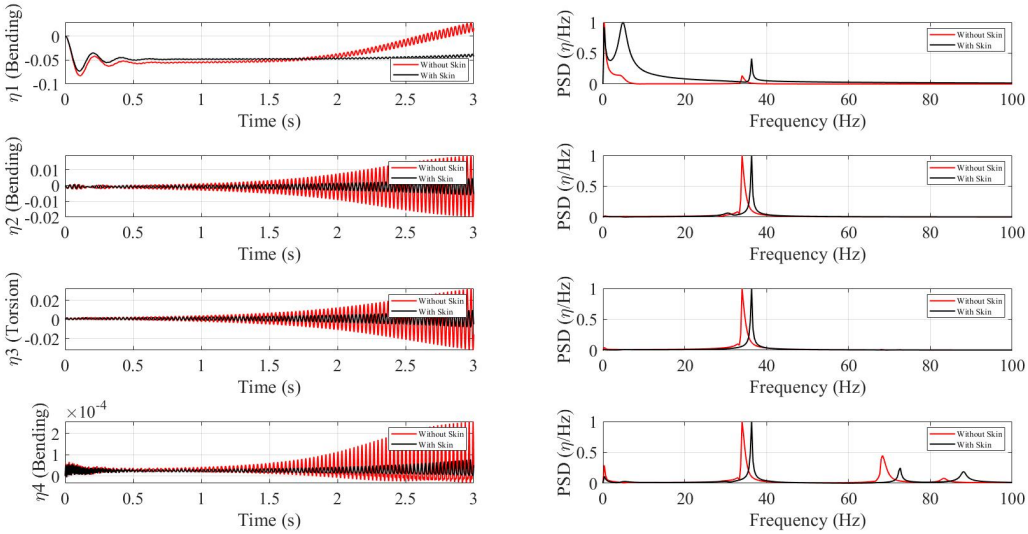

Source: Autors

Figure 6 – Time Response - Pazy Wing - $V = 60m/s$

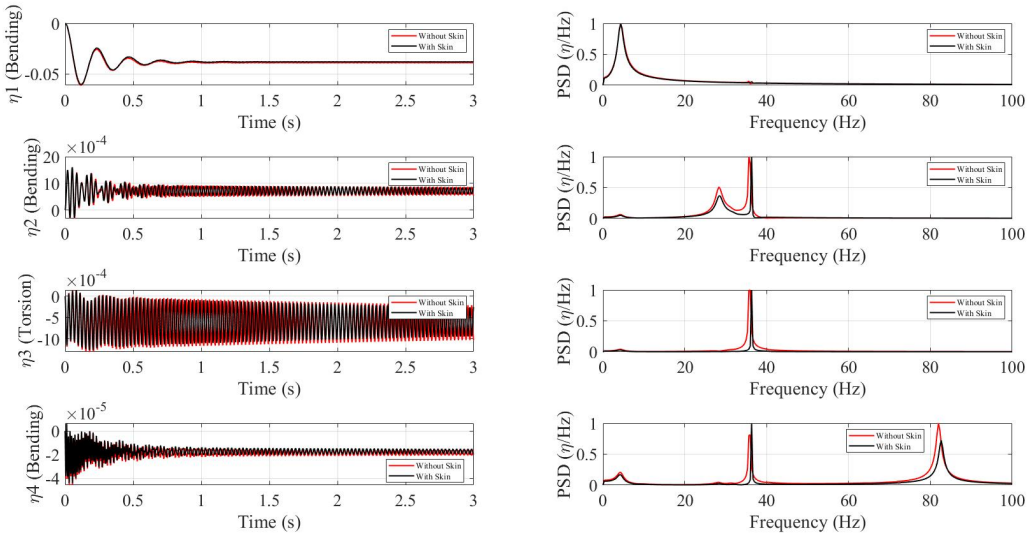

Source: Autors

The flutter speeds for the Pre-Pazy wing are in very good agreement with the literature, while lower flutter speeds were obtained for the Pazy wing, what is being investigated.

Table 3 – Flutter Speed (m/s)

		Without Skin	With Skin
PrePazy	**Present Work**	61.5	64.1
	Goizueta et al. (2021) - SHARPy	63.0	65.0
	Drachinsky and Raveh (2021) - ZAERO/MRM Model	61.8	64.4
	Drachinsky and Raveh (2021) - ZAERO/Nastran Model	-	62.4
Pazy	**Present Work**	61.3	61.77
	Riso and Cesnik (2022) - UM/NAST	-	72.40
	Riso and Cesnik (2022) - MSC Nastran	-	67.3

Figure 7 – Time Response - Pazy Wing - $V = 70m/s$

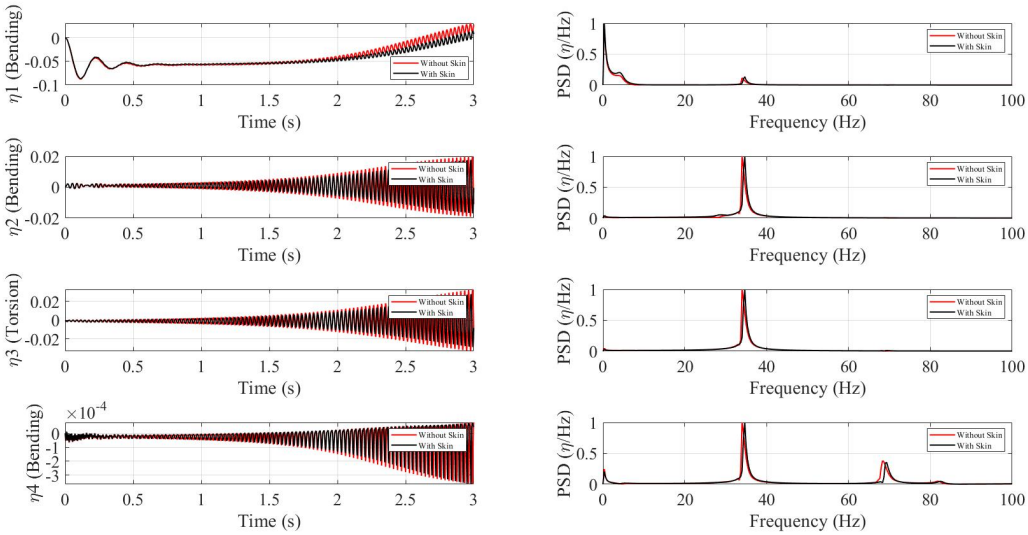

Source: Autors

Figure 8 – V-g-f - Pre-Pazy Wing

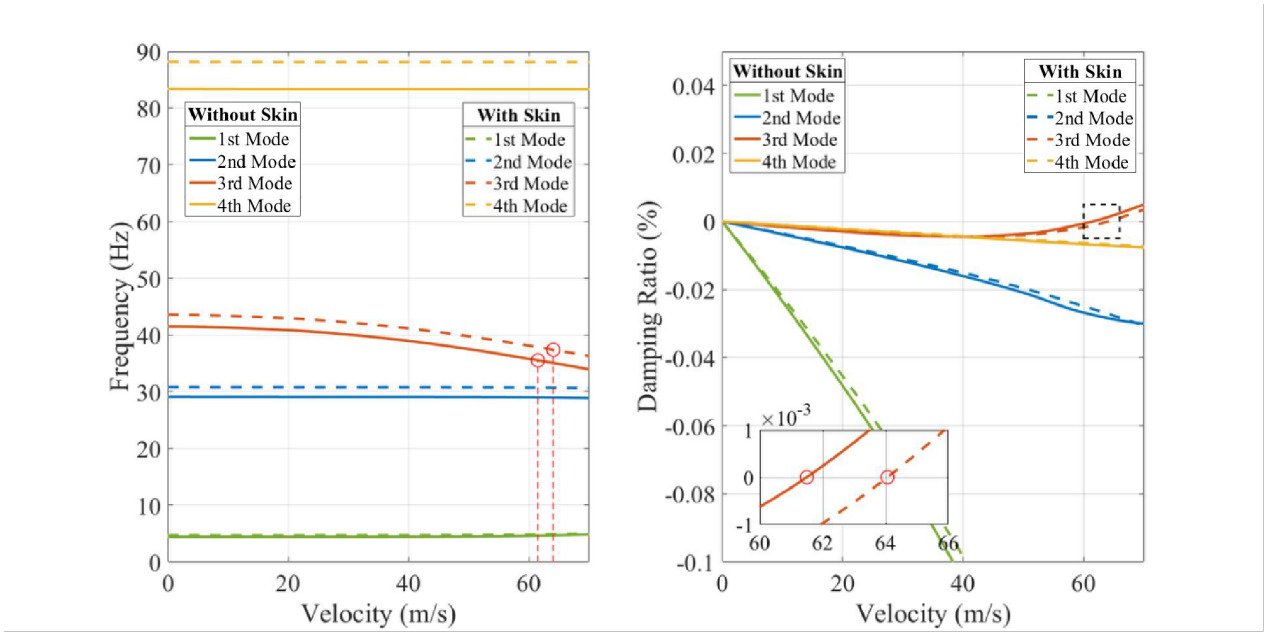

Source: Autors

Considering that the structural model applied here is a linear beam model, it's possible to say that, despite the small differences, the results presented on Table 3 have a good agreement with the ones available on the literature. Also,is important to emphasize that for the wings without skin the flutter speeds are lower to the ones obtained for the wing with skin. The skin increases the stiffness of the structure.

Despite the points highlighted here, the results obtained analyzing the Pre-Pazy and Pazy wings were quite promising. It's possible to say that all models applied here (structural, aeroelastic and system identification) have a good accuracy for the determination of natural frequencies and mode shapes, and for the flutter speed prediction. The discrepancies are being investigated and further analysis will be conducted.

ACKNOWLEDGMENTS

This study was carried out with the financial support of the Conselho Nacional de Desenvolvimento Científico e Tecnológico (National Council for Scientific and Technological Development) - CNPQ (130984/2021-3).

Figure 9 – V-g-f - Pazy Wing

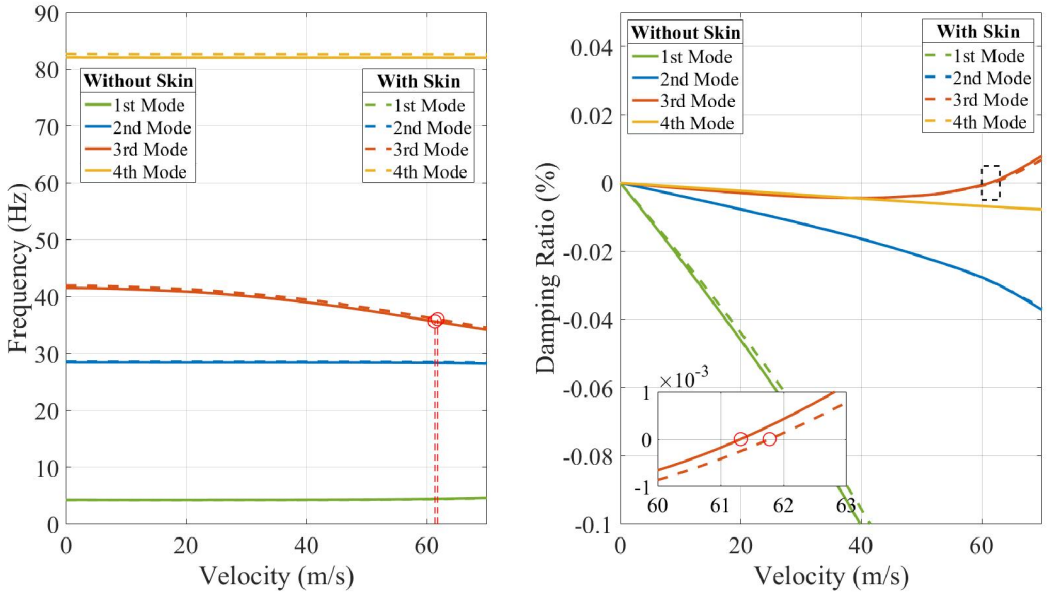

Source: Autors

REFERENCES

Avin, O., Raveh, D. E., Drachinsky, A., Ben-Shmuel, Y. and Tur, M. "An experimental benchmark of a very flexible wing.", AIAA Scitech 2021 Forum, 2021. avaible on: https://arc.aiaa.org/doi/abs/10.2514/6.2021-1709.

Benini, G. R., Belo, E. M. and Marques, F. D. "Numerical model for the simulation of fixed wings aeroelastic response." Journal of the Brazilian Society of Mechanical Sciences and Engineering [online]. 2004, v. 26, n. 2, pp. 129-136. https://doi.org/10.1590/S1678-58782004000200003.

Cook, R. and Saunders, H. "Concepts and applications of finite element analysis", 1984.

Craig, R. and Kurdila, A. "Fundamentals of Structural Dynamics." Wiley, 2006.

del Carre, A., Muñoz-Simón, A., Goizueta, N. and Palacios, R. "Sharpy: A dynamic aeroelastic simulation toolbox for very flexible aircraft and wind turbines. Journal of Open Source Software", The Open Journal, v. 4, n. 44, p. 1885, 2019. Disponível em: https://doi.org/10.21105/joss.01885.

Drachinsky, A. and Raveh, D. E. "Nonlinear Aeroelastic Analysis of Highly Flexible Wings Using the Modal Rotation Method.", AIAA Journal, 2022, Vol. 60, p. 3122-3134.

Goizueta, N., Drachinsky, A., Wynn, A., Raveh, D. E. and Palacios, R. "Flutter predictions for very flexible wing wind tunnel test.", AIAA Scitech 2021 Forum, 2021, avaible on: https://arc.aiaa.org/doi/abs/10.2514/6.2021-1711.

Guillaume, P., Verboven, P., Vanlanduit, S., Auweraer, Van der H. and Peeters, B. "A poly-reference implementation of the least-squares complex frequency-domain estimator." Proceedings of IMAC, vol. 21, 2003.

Katz, J. and Plotkin, A. "Low-speed Aerodynamics: From Wing Theory to Panel Methods." McGraw-Hill, 1991.

Katsikadelis, J. "Dynamic Analysis of Structures." Elsevier Science, 2020.

Reddy, J. N. "Introduction to the finite element method." McGraw-Hill Education, 2019.

Riso, C., Cesnik, C. E. "Correlations between um/nast nonlinear aeroelastic simulations and the pre-pazy wing experiment.", AIAA Scitech 2021 Forum, 2021, avaible on: https: //arc.aiaa.org/doi/abs/10.2514/6.2021-1712.

Riso, C., Cesnik, C. E. "Low-order geometrically nonlinear aeroelastic modeling and analysis of the pazy wing experiment.", AIAA SCITECH 2022 Forum, 2022, avaible on: https://arc.aiaa.org/doi/abs/10.2514/6.2022-2313.

Ritter, M., Hilger, J., Zimmer, M. "Static and dynamic simulations of the pazy wing aeroelastic benchmark by nonlinear potential aerodynamics and detailed FE model.", AIAA Scitech 2021 Forum, 2021, avaible on: https://arc.aiaa.org/doi/abs/10.2514/6.2021-1713.

RESPONSIBILITY NOTICE

The author(s) is (are) the only responsible for the printed material included in this paper.